

Dynamic response of a thermal transistor to time-varying signals

Qinli Ruan(阮琴丽), Wenjun Liu(刘文君), and Lei Wang(王雷)

Citation: Chin. Phys. B, 2024, 33 (**5**): 056301. DOI: 10.1088/1674-1056/ad2dcc
Journal homepage: http://cpb.iphy.ac.cn; http://iopscience.iop.org/cpb

What follows is a list of articles you may be interested in

Determining Hubbard *U* of VO_2 by the quasi-harmonic approximation

Longjuan Kong(孔龙娟), Yuhang Lu(陆雨航), Xinying Zhuang(庄新莹), Zhiyong Zhou(周志勇), and Zhenpeng Hu(胡振芃)
Chin. Phys. B, 2024, 33 (**1**): 016302. DOI: 10.1088/1674-1056/acfd18

Ab initio nonadiabatic molecular dynamics study on spin—orbit coupling induced spin dynamics in ferromagnetic metals

Wansong Zhu(朱万松), Zhenfa Zheng(郑镇法), Qijing Zheng(郑奇靖), and Jin Zhao(赵瑾)
Chin. Phys. B, 2024, 33 (**1**): 016301. DOI: 10.1088/1674-1056/acf91d

Straight and twisted Weyl nodal line phonons in Ho_2CF_2 material

Xin-Yue Kang(康鑫越), Jin-Yang Li(李金洋), and Si Li(李思)
Chin. Phys. B, 2023, 32 (**11**): 116301. DOI: 10.1088/1674-1056/aceaea

Unveiling phonon frequency-dependent mechanism of heat transport across stacking fault in silicon carbide

Fu Wang(王甫), Yandong Sun(孙彦东), Yu Zou(邹宇), Ben Xu(徐贲), and Baoqin Fu(付宝勤)
Chin. Phys. B, 2023, 32 (**9**): 096301. DOI: 10.1088/1674-1056/acdfc0

Impeded thermal transport in aperiodic BN/C nanotube superlattices due to phonon Anderson localization

Luyi Sun(孙路易), Fangyuan Zhai(翟方园), Zengqiang Cao(曹增强), Xiaoyu Huang(黄晓宇), Chunsheng Guo(郭春生), Hongyan Wang(王红艳), and Yuxiang Ni(倪宇翔)
Chin. Phys. B, 2023, 32 (**5**): 056301. DOI: 10.1088/1674-1056/acb9e7

SPECIAL TOPIC — Heat conduction and its related interdisciplinary areas

Dynamic response of a thermal transistor to time-varying signals

Qinli Ruan(阮琴丽), Wenjun Liu(刘文君), and Lei Wang(王雷)†

Department of Physics, Beijing Key Laboratory of Opto-electronic Functional Materials and Micro-nano Devices, and Key Laboratory of Quantum State Construction and Manipulation (Ministry of Education), Renmin University of China, Beijing 100872, *China*

(Received 12 January 2024; revised manuscript received 7 February 2024; accepted manuscript online 28 February 2024)

Thermal transistor, the thermal analog of an electronic transistor, is one of the most important thermal devices for microscopic-scale heat manipulating. It is a three-terminal device, and the heat current flowing through two terminals can be largely controlled by the temperature of the third one. Dynamic response plays an important role in the application of electric devices and also thermal devices, which represents the devices' ability to treat fast varying inputs. In this paper, we systematically study two typical dynamic responses of a thermal transistor, i.e., the response to a step-function input (a switching process) and the response to a square-wave input. The role of the length L of the control segment is carefully studied. It is revealed that when L is increased, the performance of the thermal transistor worsens badly. Both the relaxation time for the former process and the cutoff frequency for the latter one follow the power-law dependence on L quite well, which agrees with our analytical expectation. However, the detailed power exponents deviate from the expected values noticeably. This implies the violation of the conventional assumptions that we adopt.

Keywords: phonon, phononics, thermal transistor, dynamic response, heat conduction

PACS: 63.22.–m, 63.20.–e, 44.10.+i, 05.70.Ln **DOI:** 10.1088/1674-1056/ad2dcc

1. introduction

With the advancement of micro-electronics, the design and manufacture of nanoelectronic devices have been rapidly developed and have broadly facilitated many aspects of our daily life. The potential of applying microscopic heat control may result in comparable wealth of applications. In the past period, phononics, a new science and engineering manipulating heat flow with electronic analogs, has been put forward greatly.[1] Analogous to the electric components, two fundamental thermal devices, the thermal diode[2] with rectification of heat flux and the thermal transistor[3] with the control of heat transport, have been proposed. The thermal transistor is used to operate thermal switching, thermal amplification, thermal logic,[4] and thermal storage.[5] For its fundamentality and versatility, it is often cited as the backbone of thermal circuits. Over the years, various thermal transistors based on near-field thermal radiation,[6] nonlinear phonon conduction in nanoscale systems,[7,8] nanoscale confined fluids, quantum electronic systems,[9–13] and Josephson junction between different superconductors[14,15] have been designed and some of them have been experimentally demonstrated.[16–21] In many cases, with the help of a suitably designed electromagnetic field, the thermal control functions can be realized more easily.

The above studies mostly focus on the systems in stationary states. The nonstationary properties, however, have not received enough attention yet. Commonly, systems in nonstationary and stationary states behave quite differently. The parabolic Fourier equation, which is a law for stationary-state heat conduction, implies infinite speed of the signal propagation, thus it is inconsistent with causality and cannot well describe nonstationary-state heat conduction. The Cattaneo–Vernotte law[22,23] has then been proposed to recover it. The local thermal equilibrium (LTE), which is a basic assumption for linear response theory, might also be broken in heat diffusion processes induced by even infinitesimal perturbation.[24] In a fast-varying temperature field, the generally applied quasistatic assumption in conventional statistical mechanics becomes invalid. A physical quantity, e.g., heat current, caused by a time-varying driving no longer equals its temporal average of static values, and additional geometric contribution must be considered.[25–27] Recently, rich and significant physical phenomena have been presented in systems with time-varying driving, such as the heat pump induced by geometric heat flux,[28] heat transport in the forbidden band gap of a nonlinear chain,[29] and the ratchet heat flux against thermal bias[30–33] or under zero average thermal bias.[33–35]

In the practical point of view, due to the capacitance at the PN junction, an electric diode loses its rectification function to high-frequency signals badly. The case for electric transistor is similar. Easy to understand, the performance of thermal control devices will also be largely affected by the frequency of input signals. The high-frequency-induced performance loss has already been observed for a model of thermal diode.[36] Beyond that, there are still very few studies on the dynamic response of this or other heat control devices, in particular the thermal transistor. Such studies help design thermal devices with optimal performance in operating fast-varying inputs.

†Corresponding author. E-mail: phywanglei@ruc.edu.cn

© 2024 Chinese Physical Society and IOP Publishing Ltd

In this paper, we focus on the dynamic response, the response to time-varying signals, of this key thermal device, the thermal transistor. The rest of the paper is organized as follows. Section 2 is devoted to the introduction for the model of thermal transistor. Section 3 presents two types of dynamic response of this thermal transistor. Both numerical simulations and theoretical analyses will be provided. Discussion and conclusion are represented in Section 4.

2. Model of the thermal transistor

Analogous to an electric field effect transistor, a thermal transistor consists of three terminals, source (S), drain (D), and gate (G). The function is that when a constant temperature drop is applied between the terminals D and S, the heat current flows from D to S is sensitively controlled by the temperature of the terminal G. A model that realizes such a function was first proposed in the year 2005.[3] The central part of the model is a weak interface and the power spectra at the interface depend on the temperature sensitively. The so induced match and mismatch of power spectra at the interface induce a sensitive temperature dependence of interfacial heat resistance. The negative differential thermal resistance (NDTR), the key factor of a thermal transistor, is thus realized. Various theoretical models to realize NDTR with quite different underlying mechanisms have been proposed in recent years.[37–40] The above underlying mechanism is, however, still one of the most efficient.

Here we study the dynamic response of a model of thermal transistor based on this mechanism. The model consists of three weakly coupled Frenkel–Kontorova (FK)[40] segments. The FK model is a highly simplified model that describes a crystalline solid derived from the coupling between the film material and the substrate material. The setup is illustrated in Fig. 1 and the corresponding Hamiltonian for the whole system follows:

$$\begin{aligned} H &= H_{\rm S}+H_{\rm D}+H_{\rm G}+H_{\rm int}+H_{\rm int_G} \\ &= \sum_{i=1}^{N_{\rm S}} \frac{1}{2}\dot{x}_{{\rm S},i}^2+\frac{1}{2}k_{\rm S}(x_{{\rm S},i}-x_{{\rm S},i-1})^2-\frac{V_{\rm S}}{(2\pi)^2}\cos 2\pi x_{{\rm S},i} \\ &\quad+\sum_{i=1}^{N_{\rm D}} \frac{1}{2}\dot{x}_{{\rm D},i}^2+\frac{1}{2}k_{\rm D}(x_{{\rm D},i}-x_{{\rm D},i-1})^2-\frac{V_{\rm D}}{(2\pi)^2}\cos 2\pi x_{{\rm D},i} \\ &\quad+\sum_{i=1}^{N_{\rm G}} \frac{1}{2}\dot{x}_{{\rm G},i}^2+\frac{1}{2}k_{\rm G}(x_{{\rm G},i}-x_{{\rm G},i-1})^2-\frac{V_{\rm G}}{(2\pi)^2}\cos 2\pi x_{{\rm G},i} \\ &\quad+\frac{1}{2}k_{\rm int}(x_{{\rm S},N_{\rm S}}-x_{{\rm D},N_{\rm D}})^2+\frac{1}{2}k_{\rm int_G}(x_{{\rm S},N_{\rm S}}-x_{{\rm G},N_{\rm G}})^2, \end{aligned} \quad (1)$$

where $x_{{\rm D},i}$, $x_{{\rm S},i}$, and $x_{{\rm G},i}$ denote the particles' displacements from their equilibrium positions in the three segments D, S, and G, respectively. The mass of each particle has been set to unity. Fixed boundary conditions (BC) are taken for all the three segments, i.e., $x_{{\rm D},0}=x_{{\rm S},0}=x_{{\rm G},0}=0$. To reduce the boundary effect of the G segment, the input heat bath will be attached to not the end particle of this segment but a particle at a shorter distance $L \le N_{\rm G}$. Basically, only the heat resistance in this part plays a noticeable role, thus L instead of $N_{\rm G}$ is called the length of the segment G hereafter. We have confirmed that such a change affects the results very slightly. Unless otherwise stated, the parameters of the thermal transistor are $N_{\rm D}=N_{\rm S}=4$, $N_{\rm G}=200$, $T_{\rm D}=0.2$, $k_{\rm D}=0.05$, $V_{\rm D}=0$, $k_{\rm int}=0.06$, $T_{\rm S}=0.04$, $k_{\rm S}=0.2$, $V_{\rm S}=6.0$, $k_{\rm G}=1.0$, $V_{\rm G}=5.0$, and $k_{\rm int_G}=1.0$. The so chosen parameters guarantee that the thermal transistor works well as a thermal switch in a wide regime of L, and they are all in the experimentally accessible regime. The correspondence between the real physical quantities and the dimensionless ones we applied can be found in Ref. [42].

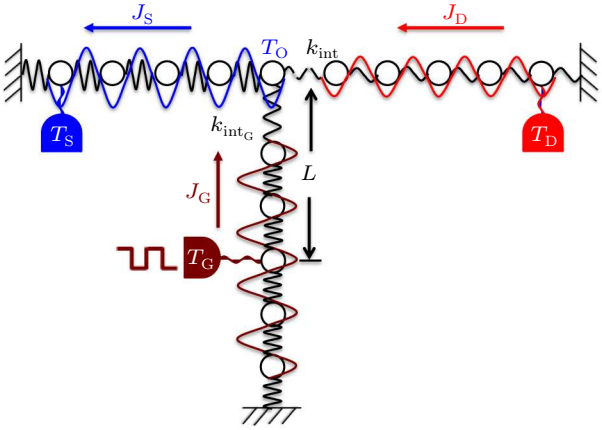


Fig. 1. Configuration of the thermal transistor. The device consists of three Frenkel–Kontorova type segments, D, S, and G. For fixed $T_{\rm D}$ and $T_{\rm S}$ ($T_{\rm D}>T_{\rm S}$), $J_{\rm D}$ and $J_{\rm S}$ depend sensitively on the temperature $T_{\rm O}$, which is controlled by $T_{\rm G}$. Unlike in our previous studies, the control heat bath $T_{\rm G}$ is attached not to the end particle of segment G but to a particle with a shorter distance L.

3. Dynamic response of the thermal transistor

3.1. Fundamental diagram

First of all, the fundamental diagram of the thermal transistor, i.e., the stationary-state heat currents $J_{\rm D}$ and $J_{\rm S}$ versus the temperature $T_{\rm O}$, is calculated. To do that, the temperatures $T_{\rm D}$, $T_{\rm S}$ and $T_{\rm O}$ are fixed to required values. After a transient time typically 10^7 time units, the system approaches a stationary state, i.e., all the local temperatures become time independent and the heat current in each segment becomes also site independent. Then the values of the heat currents are measured and plotted in Fig. 2. We see in a quite wide regime of $T_{\rm O}$, the heat current $J_{\rm D}$ increases with decreasing temperature difference in this segment $T_{\rm D}-T_{\rm O}$. This is the so called NDTR. $J_{\rm D}$ and $J_{\rm S}$ can thus equal each other at three different states, 'on', 'semi-on' and 'off' states, for which $T_{\rm O}=T_{\rm off}$ ($=0.04$), $T_{\rm O}=T_{\rm semi\text{-}on}$ ($=0.07$), and $T_{\rm O}=T_{\rm on}$ ($=0.163$), respectively. The function of a thermal switch is thus realized.[3]

Ideally speaking, if the input signal can be directly injected into the particle O, then the performance of the thermal transistor reaches its best. It is, however, practically impossible since the particle O is located inside the device. That is why a control segment G must be considered. As we have already proven, when the effective length of the segment G is not too long, the thermal transistor is controllable, i.e., for any given value of $T_{\rm G} \in [T_{\rm off}, T_{\rm on}]$ there exists only one value of stationary-state $T_{\rm O}$.[43] Throughout this paper, we study such cases only.

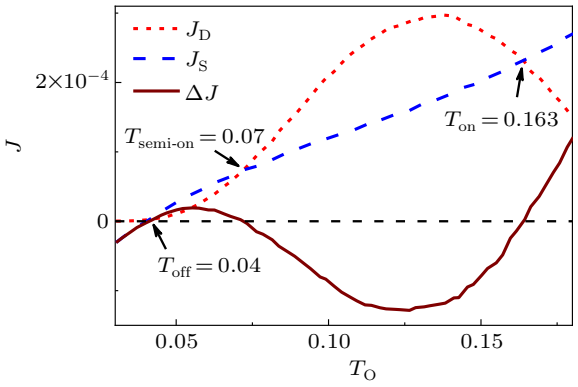


Fig. 2. Fundamental diagram of the thermal transistor. Stationary-state heat currents $J_{\rm D}$, $J_{\rm S}$ and $\Delta J \equiv J_{\rm S} - J_{\rm D}$ versus the temperature $T_{\rm O}$ are plotted. In the three key states $T_{\rm O} = T_{\rm off} = 0.04$, $T_{\rm O} = T_{\rm semi\text{-}on} = 0.07$, and $T_{\rm O} = T_{\rm on} = 0.163$, ΔJ equals zero exactly.

3.2. Switching processes

One of the main functions of the thermal transistor is thermal switching,[3] which is a basis of many other complicated functions such as thermal logic gates[4] and thermal memory.[5] Here we study the dynamic switching processes, i.e., the 'on–off' and 'off–on' processes, in a thermal transistor. To simulate an 'on–off' process, a heat bath with temperature $T_{\rm G} = T_{\rm on}$ is initially attached to the segment G for enough long time so as to set $T_{\rm O}$ and the temperature of the whole segment G to $T_{\rm on}$. At the time $t = 0$, the temperature $T_{\rm G}$ is switched to $T_{\rm off}$. Then the system will asymptotically approach the 'off' state, i.e., $T_{\rm O}$ and the temperature of the whole segment G approach $T_{\rm off}$. An 'off–on' process is similar.

The 'on–off' and 'off–on' processes are numerically simulated for a model of thermal transistor with very different lengths of segment G, $L = 10$ and 200. To indicate how close the system approaches the asymptotic states, we define the relative temperatures of the particle O,

$$\Delta T_+ \equiv \frac{T_{\rm O} - T_{\rm off}}{T_{\rm on} - T_{\rm off}}, \tag{2}$$

$$\Delta T_- \equiv \frac{T_{\rm on} - T_{\rm O}}{T_{\rm on} - T_{\rm off}}, \tag{3}$$

for the 'on–off' and 'off–on' processes, respectively. They are initially unity and asymptotically approach zero in the corresponding processes.

The numerically obtained ΔT_+ and ΔT_- versus time t during the processes are plotted in Figs. 3(a) and 3(b). We see that in the main part of the processes, they follow exponential decays with the exponents η_+ and η_-, respectively, i.e., for the 'on–off' process

$$\Delta T_+ \sim {\rm e}^{-\eta_+ t}, \tag{4}$$

and likewise for the 'off–on' process

$$\Delta T_- \sim {\rm e}^{-\eta_- t}. \tag{5}$$

To understand such universal exponential decays, we study the evolution of the system during the operation processes. For an 'on–off' process, we have observed that the system spends most of the time on the states that are very close to the asymptotic state, the 'off' state. This fact enables us to concentrate on the close-to-off part only.

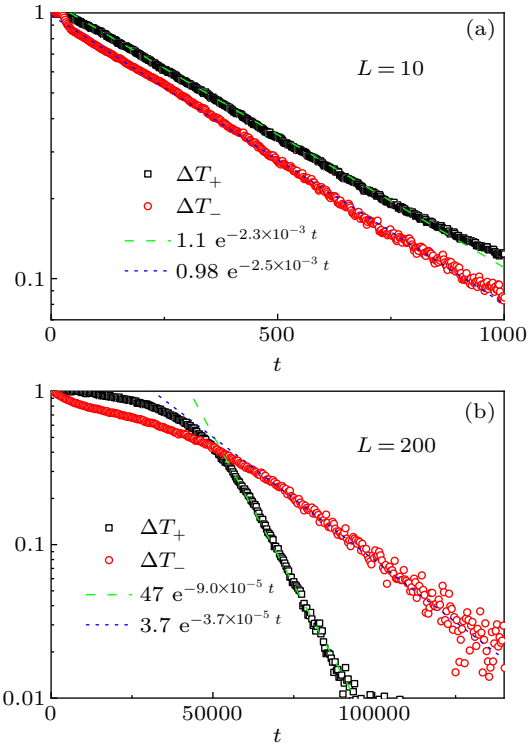


Fig. 3. The switching processes of a thermal transistor. The relative temperatures $\Delta T_\pm$ for (a) $L = 10$ and (b) $L = 200$. In both cases, ΔT_+ and ΔT_- follow exponential decays with time t asymptotically, which is expected by the Eqs. (15) and (16).

To make a theoretical analysis, we have to apply all the conventional assumptions, including the Fourier law of heat conduction, LTE, and quasistatic. When $T_{\rm O}$ is sufficiently close to $T_{\rm off}$, the dynamics of the local temperature distribution $T(x,t)$ along the G segment can be described by the following linear differential equation:

$$\frac{\partial \theta(x,t)}{\partial t} = \frac{\kappa_{\rm off}}{c_{\rm off}} \frac{\partial^2 \theta(x,t)}{\partial x^2}, \tag{6}$$

where x denotes the displacement relative to the heat bath, i.e., $x = L$ for the particle O and $x = 0$ for the particle coupled to the heat bath. $\theta(x,t) \equiv T(x,t) - T_{\rm off}$, and $c_{\rm off}$ and $\kappa_{\rm off}$ denote the

specific heat and the thermal conductivity of the G segment at temperature $T_{\rm off}$, respectively.

For $t>0$, the following boundary conditions hold:

$$\theta(0,t)=0, \tag{7}$$

$$-\kappa'_{\rm off}\theta(L,t)+\kappa_{\rm off}\frac{\partial\theta(x,t)}{\partial x}|_{x=L}=0, \tag{8}$$

where $\kappa'_{\rm off}\equiv\kappa^{\rm D}_{\rm off}+\kappa^{\rm S}_{\rm off}$, $\kappa^{\rm D}_{\rm off}\equiv\frac{{\rm d}J_{\rm D}}{{\rm d}T_{\rm O}}|_{T_{\rm O}=T_{\rm off}}$, and $\kappa^{\rm S}_{\rm off}\equiv-\frac{{\rm d}J_{\rm S}}{{\rm d}T_{\rm O}}|_{T_{\rm O}=T_{\rm off}}$. According to the stability conditions, both $\kappa'_{\rm off}$ and $\kappa'_{\rm on}$ must be positive. Hereafter, all the subscripts 'off' of the variables κ, c, and κ' are omitted for simplification.

Considering the initial condition

$$\theta(L,0)=T_{\rm on}-T_{\rm off}, \tag{9}$$

the solutions of the Eq. (6) take the form of

$$\theta(x,t)=\sum_m C_m\sin\left(\frac{\mu_m x}{L}\right)\exp\left(-\frac{\kappa\mu_m^2}{cL^2}t\right), \tag{10}$$

where μ_m satisfies

$$\tan(\mu_m)=\frac{\kappa}{\kappa' L}\mu_m. \tag{11}$$

Since $\sin[\mu_m(x/L)]$ is an odd function of x and $\sin(0)=0$, we may consider positive values of μ_m only. Furthermore, because we are interested in the asymptotic behaviour of the system, we take only the lowest positive term μ_1, which corresponds to the mode that decays the most slowly. The coefficient C_1 reads

$$C_1=\frac{T_{\rm on}-T_{\rm off}}{N(\mu_1)}\int_0^L\sin\left(\frac{\mu_1 x}{L}\right){\rm d}x, \tag{12}$$

where

$$N(\mu_1)\equiv\int_0^L\sin^2\left(\frac{\mu_1 x}{L}\right){\rm d}x=-\frac{\sin(2\mu_1)L}{4\mu_1}+\frac{L}{2}. \tag{13}$$

Therefore,

$$\theta(x,t)=\frac{4(T_{\rm on}-T_{\rm off})(1-\cos\mu_1)}{-\sin(2\mu_1)+2\mu_1}\sin\left(\frac{\mu_1 x}{L}\right)\exp\left(-\frac{\kappa\mu_1^2}{cL^2}t\right). \tag{14}$$

In the short L limit, $\mu_1\to\pi/2$, the relative temperature ΔT_+ of the particle O ($x=L$) follows:

$$\Delta T_+\equiv\frac{\theta(L,t)}{T_{\rm on}-T_{\rm off}}=\frac{4}{\pi}\exp\left(-\frac{\kappa\pi^2}{4cL^2}t\right). \tag{15}$$

In the long L limit, $\mu_1\to\pi+(\pi\kappa/\kappa' L)+O(1/L^2)$. Therefore,

$$\Delta T_+\equiv\frac{\theta(L,t)}{T_{\rm on}-T_{\rm off}}=\frac{4\kappa}{\kappa' L}\exp\left(-\frac{\kappa\pi^2}{cL^2}t\right). \tag{16}$$

Equations (15) and (16) well explain the above observed exponential decay of ΔT_+ as shown in Fig. 3. The same derivations also apply to the 'off–on' process thus the exponential decay of ΔT_- can be explained in the same way.

However, something unexpected has also been revealed. First, at the beginning of the process, the decays look much slower. This can be observed clearly in the $L=200$ case, see Fig. 3(b). It can be understood by the stability of the initial state, 'on' or 'off'. Namely, around the 'on' or 'off' state when small perturbation causes a change of $T_{\rm O}$, the induced net heat current will push $T_{\rm O}$ back.[5] This makes the Eq. (6), which applies to the asymptotic state, invalid. More importantly, the detailed dependence of the exponents η_- and η_+ on the length L does not agree with the expectation. In Fig. 4, the numerically obtained η_+ and η_- versus L are plotted. They both follow power-law decays with L, the detailed power exponents are -1.15 and -1.4, which differ from the expected value of -2 apparently. The reasons might be the following. (i) In the physical aspect, the assumptions of Fourier law, LTE, and quasistatic are in fact not well satisfied in such a small and fast-varying system. We have numerically observed that the Fourier law of heat conduction in the G segment is broken down, i.e., the heat conductivity is not a length-independent constant but diverges with the length L by L^α with $\alpha>0$, just like what is commonly observed in 1D lattices with momentum-conservation.[44–46] In such cases, the local heat current can no longer be determined by the local quantities, e.g., the local temperature and local temperature gradient, alone. A quantitative calculation becomes much more complicated. Nevertheless, qualitatively speaking, the heat resistance in the segment G increases not as fast as L^1, but follows $L^{1-\alpha}$ with positive α only, thus the role of the length L is weakened greatly. The above discrepancy can be mostly attributed to it. The effects of the breakdown of the other assumptions are even harder to figure out. They might be considered in future studies. (ii) In the mathematical aspect, the Eqs. (15) and (16) are for the short and long L limits, respectively. There exists a factor 4 in the denominator of the exponent in the Eq. (15), which indicates a slowdown of the decay of η in the medium length L.

Furthermore, to quantitatively measure the performance of the thermal switch, we define a relaxation time $t_{\rm c}$ at which the ΔT decays to a critical value $1/{\rm e}$,

$$\Delta T_\pm(t_{\rm c\pm})=\frac{1}{\rm e}. \tag{17}$$

Compared with the values of $\eta_\pm$ which describe the asymptotic part of a switching process only, the relaxation time measures the entire process more precisely. In the ideal case that $\Delta T_\pm\sim{\rm e}^{-\eta_\pm t}$ throughout the whole switching process and $\eta_\pm\sim L^{-2}$, simply $t_{\rm c\pm}\sim L^2$. The numerically measured relaxation time $t_{\rm c+}$ and $t_{\rm c-}$ are plotted in Fig. 4(b). They both follow a power-law growth with L. This reveals quantitatively the high importance of reducing the thermal resistance in the

G segment. The shorter the G segment is, the faster the operation processes can be completed. Not surprisingly, the detailed power-exponents do not agree with the above expected value 2 very well.

In the above simulations, the lengths of the D and S segments N_D and N_S are always fixed to a relatively short value 4. To observe the universality of the above conclusions, we have also simulated systems for longer N_D and N_S. In Fig. 5, the switching processes for $N_D = N_S = 50$ and 200 are presented. In all the cases, exponential decays of ΔT can be clearly confirmed. The relaxation time also follows power-law divergence quite well, although the detailed power exponents may vary.

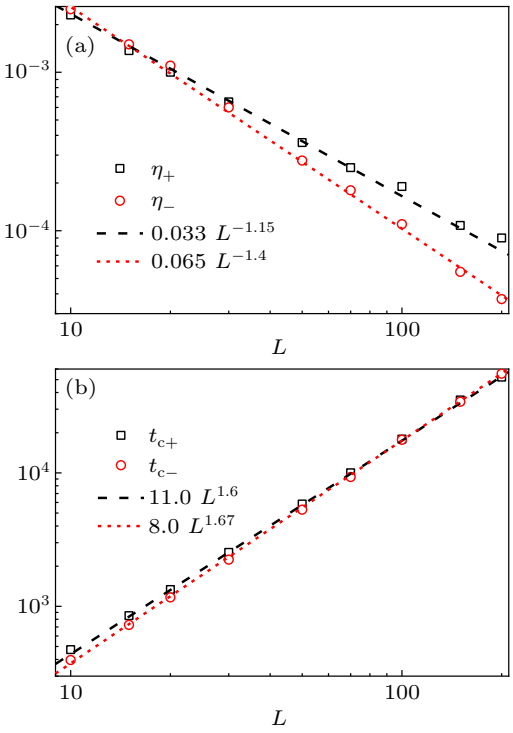


Fig. 4. (a) Exponents η_+ and η_- for 'on–off' and 'off–on'. The decays of η_+ and η_- satisfy the power law. (b) The relaxation time t_{c+} and t_{c-}, the time it takes for $\Delta T_\pm$ to fall to $1/e$, are plotted.

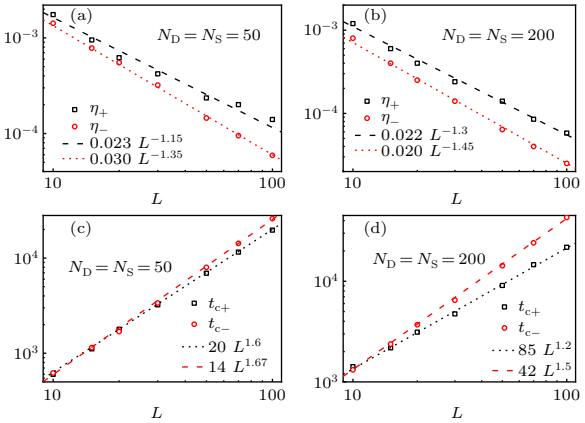


Fig. 5. The exponents $\eta_\pm$ and relaxation time $t_{c\pm}$ for the 'on–off' and 'off–on' processes. Left column, $N_D = N_S = 50$. Right column, $N_D = N_S = 200$.

3.3. Response to periodic inputs

Next, we study the frequency response, i.e., the response of the thermal transistor to a periodic input signal. It measures more precisely the performance of a thermal device under a fast varying input signal. Here we study the simplest case, in which the input temperature T_G takes the form of a square wave,

$$T_G = T_0(1+\Delta), \tag{18}$$

$$\Delta = A\,\mathrm{sgn}\left(\sin\frac{2\pi t}{P}\right). \tag{19}$$

We set the mean input temperature $T_0 = (T_{on}+T_{off})/2$ and the oscillation amplitude $A = (T_{on}-T_{off})/2$, thus T_G jumps between T_{on} and T_{off} periodically. After the T_G oscillates enough rounds, all other modes vanish and the whole system reaches a periodic state whose period equals that of the external driving P. In such a case, we need only to study the periodic variation of any quantity within a full temporal period.

The calculated $T_O(P,\tau)$ versus the rescaled time,

$$\tau \equiv \frac{t}{P} \tag{20}$$

for four representative values of P are plotted in Fig. 6(a). Each plotted value is an average over 10^4 to 10^7 temporal periods, which consist of about 4×10^9 time units. In the very long P case, say, $P = 4\times10^5$, the corresponding $T_O(P,\tau)$ basically forms a square wave. For a not very long P, say $P = 1\times10^4$, $T_O(P,\tau)$ changes gradually from T_{on} to T_{off} and keeps there a while, and then changes back to T_{on} and keeps. For even shorter P, say $P = 2\times10^3$, the above required transient time is too long thus T_{on} and T_{off} can no longer be reached. $T_O(P,\tau)$ can oscillate only in a narrower regime. For a very short P, say $P = 4\times10^2$, T_O keeps basically static. Correspondingly, the heat currents $J_D(P,\tau)$, $J_S(P,\tau)$, and $J_G(P,\tau)$ are plotted in Figs. 6(b)–6(d), respectively. These figures illustrate how badly the performance of the thermal transistor is affected by the frequency of the input signal.

To measure the performance of the thermal transistor more precisely, we calculate the standard deviation of $T_O(P,\tau)$,

$$\sigma[T_O(P,\tau)] \equiv \sqrt{\int_0^1 [T_O(P,\tau) - \langle T_O(P,\tau)\rangle]^2\,\mathrm{d}\tau}, \tag{21}$$

where

$$\langle T_O(P,\tau)\rangle \equiv \int_0^1 T_O(P,\tau)\,\mathrm{d}\tau \tag{22}$$

denotes the average of $T_O(P,\tau)$. In the long P limit, as we have observed, $T_O(P,\tau)$ jumps between T_{on} and T_{off} periodically, thus

$$\sigma[T_O(\infty,\tau)] = \frac{T_{on}-T_{off}}{2}. \tag{23}$$

While in the short P limit, $T_{\rm O}(P,\tau)$ becomes a τ-independent constant thus $\sigma[T_{\rm O}(P,\tau)]$ approaches zero, which indicates explicitly that the output can no longer be controlled by the input. Therefore, the relative standard deviation

$$\gamma(P) \equiv \frac{\sigma[T_{\rm O}(P,\tau)]}{\sigma[T_{\rm O}(\infty,\tau)]} \tag{24}$$

takes a value within the interval $(0,1)$ and it quantitatively describes the control ability of the transistor to the periodically-varying input signal.

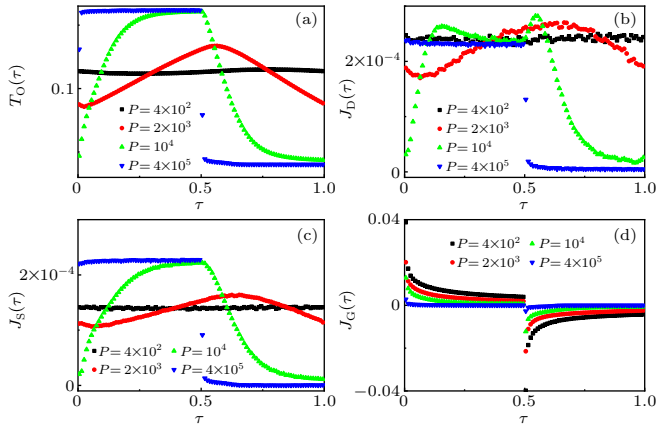


Fig. 6. The periodic temperature $T_{\rm O}$ and the periodic asymptotic local heat currents $J_{\rm D/S/G}$ flowing from the heat bathes $T_{\rm D/S/G}$ versus the rescaled phase τ for $L=20$. Data binning over contiguous τ regimes has been performed in order to reduce statistical fluctuations.

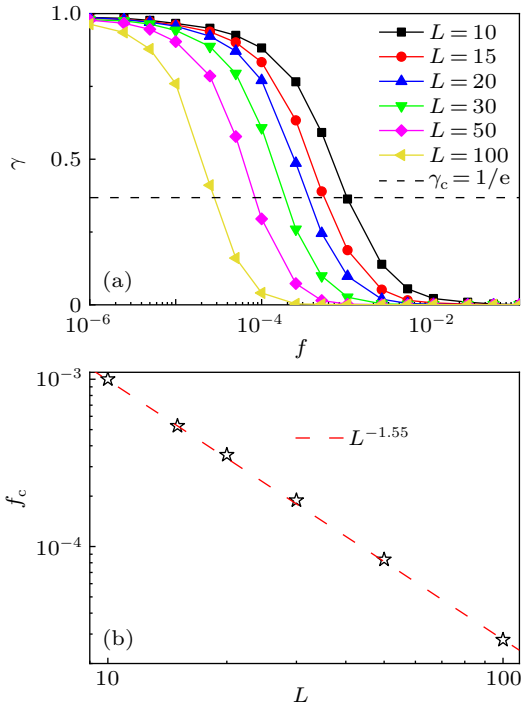


Fig. 7. (a) The relative standard deviation γ versus the input frequency f for various lengths of G segment L. The horizontal dashed line stands for $\gamma=\gamma_{\rm c}=1/{\rm e}$. (b) The cutoff frequency $f_{\rm c}$ versus L. A red dashed line with slop -1.55 is plotted for reference.

The $\gamma(P)$ versus the input frequency $f=1/P$ of this thermal transistor for various L is plotted in Fig. 7(a). As expected, in all cases $\gamma(P)$ decays with f gradually, and the longer the L the faster the decay. To quantitatively measure whether the thermal transistor is still able to operate the high-frequency input, a cutoff frequency $f_{\rm c}$ is defined as the value of input frequency for which γ decays to a critical value $\gamma_{\rm c}$, i.e.,

$$\gamma\left(\frac{1}{f_{\rm c}}\right) \equiv \gamma_{\rm c}. \tag{25}$$

Here we set $\gamma_{\rm c}=1/{\rm e}\approx0.36788$. The so calculated $f_{\rm c}$ versus the length L is plotted in Fig. 7(b). It follows a power-law dependence with L, i.e., $f_{\rm c}\sim L^{-1.55}$ quite well. Compared with the switching processes, the theoretical analyses for this process are even more difficult. Besides the validity problems of the conventional assumptions, unlike in a switching process in which all the heat conductivities and specific heat can be treated as constants since we are interested in the asymptotic states only, here they are local temperature dependent. The Eqs. (6) and (8) become much more complicated. In such a case, we conjecture the above power exponent should equal -2, just like the one expected in a thermal diode model.[30] The discrepancy can be mainly attributed to the anomalous heat conduction in the G segment again.

4. Discussion and summary

The dynamic response of a thermal transistor under time-varying input signals has been systematically studied. The roles of the length L of the G segment have been investigated particularly. First, in the switching processes, exponential decays to the asymptotic states are clearly observed, and the exponents satisfy power-law scalings with L in all cases. These findings agree with our theoretical analyses. The detailed scaling power exponents, however, differ from the expectations largely. The relaxation time $t_{\rm c}$ of the thermal transistor, the time that the transistor spends on completing the switch processes, is also measured. The case is similar, i.e., the power-law scaling with L can be correctly predicted, however, the detailed values of the power exponents deviate noticeably from the predictions.

Second, the frequency response of the thermal transistor to a square-wave signal is investigated. The control ability of the transistor can be represented by the standard deviation of the key temperature $T_{\rm O}$ under the periodic input. As expected, when the frequency of the input signal increases, the ability is lost gradually, and the longer the L is the more rapidly the loss enlarges. A critical frequency $f_{\rm c}$ can be naturally defined as the value, at which the performance of the thermal transistor vanishes to an unacceptable level. We reveal numerically that $f_{\rm c}$ follows a power-law decay with L, i.e., $f_{\rm c}\sim L^{-1.55}$. The important role of the heat resistance in the control segment is clearly presented. Compared with the switching processes, theoretical analyses for the frequency response are even more difficult.

This study may help designing thermal transistors that realize various heat control functions in rapidly changing conditions and broaden their applications. To the best of our knowledge, such studies are still very rarely reported. The theoretical part of the study is still quite preliminary. We have to apply many conventional assumptions, which are in fact not well satisfied in such a few-particle, far-from-equilibrium, and fast-varying system. That is why the agreement with the numerical observations is not satisfying. The types of the decay and growth, exponential or power law, have been obtained successfully. However, very noticeable discrepancies in the detailed values of exponent and power still exist. More intensive studies are necessary before we can understand the findings and determine the scaling properties more exactly.

Acknowledgments

Project supported by the National Natural Science Foundation of China (Grant No. 12075316), the Fundamental Research Funds for the Central Universities, and the Research Funds of Renmin University of China (Grant No. 21XNH091) (Q.R.). Computational resources were provided by the Physical Laboratory of High Performance Computing at Renmin University of China.

References

[1] Li N, Ren J, Wang L, Zhang G, Hänggi P and Li B 2012 *Rev. Mod. Phys.* **84** 1045
[2] Terraneo M, Peyrard M and Casati G 2002 *Phys. Rev. Lett.* **88** 094302
[3] Li B, Wang L and Casati G 2006 *Appl. Phys. Lett.* **88** 143501
[4] Wang L and Li B 2007 *Phys. Rev. Lett.* **99** 177208
[5] Wang L and Li B 2008 *Phys. Rev. Lett.* **101** 267203
[6] Ben-Abdallah P and Biehs S A 2014 *Phys. Rev. Lett.* **112** 044301
[7] Defaveri L, Almeida A A A and Anteneodo C 2023 *Phys. Rev. E* **108** 044126
[8] Dmitriev S V, Kuzkin V A and Krivtsov A M 2023 *Phys. Rev. E* **108** 054221
[9] Ren J and Zhu J X 2013 *Phys. Rev. B* **87** 241412
[10] Joulain K, Drevillon J, Ezzahri Y and Ordonez-Miranda J 2016 *Phys. Rev. Lett.* **116** 200601
[11] Guo B Q, Liu T and Yu C S 2018 *Phys. Rev. E* **98** 022118
[12] Guo B Q, Liu T and Yu C S 2019 *Phys. Rev. E* **99** 032112
[13] Liu H, Wang C, Wang L Q and Ren J 2019 *Phys. Rev. E* **99** 032114
[14] Fornieri A, Timossi G, Bosisio R, Solinas P and Giazotto F 2016 *Phys. Rev. B* **93** 134508
[15] Khomeriki R, Lepri S and Ruffo S 2004 *Phys. Rev. E* **70** 066626
[16] Ng R C, Castro Alvarez A and Sotomayor Torres C M 2022 *Energies* **15** 4685
[17] Castelli L, Zhu Q, Shimokusu T J and Wehmeyer G 2023 *Nat. Commun.* **14** 393
[18] Xie R, Bui C T, Varghese B, Zhang Q, Sow C H, Li B and Thong J T L 2011 *Adv. Funct. Mater.* **21** 1602
[19] Dyakov S A, Dai J, Yan M and Qiu M 2015 *J. Phys. D* **48** 305104
[20] Ito K, Nishikawa K and Iizuka H 2016 *Appl. Phys. Lett.* **108** 053507
[21] Morsy A M, Biswas R and Povinelli M L 2019 *APL Photonics* **4** 010804
[22] Christov C I and Jordan P M 2005 *Phys. Rev. Lett.* **94** 154301
[23] Gendelman O V and Savin A V 2010 *Phys. Rev. E* **81** 020103
[24] Wang L, Liu S and Li B 2019 *New J. Phys.* **21** 083019
[25] Esposito M, Harbola U and Mukamel S 2009 *Rev. Mod. Phys.* **81** 1665
[26] Jarzynski C and Wójcik D K 2004 *Phys. Rev. Lett.* **92** 230602
[27] Saito K and Dhar A 2007 *Phys. Rev. Lett.* **99** 180601
[28] Ren J, Hänggi P and Li B 2010 *Phys. Rev. Lett.* **104** 170601
[29] Geniet F and Leon J 2002 *Phys. Rev. Lett.* **89** 134102
[30] Li N, Hänggi P and Li B 2008 *Europhys. Lett.* **84** 40009
[31] Ordonez-Miranda J, Anufriev R, Nomura M and Volz S 2022 *Phys. Rev. B* **106** L100102
[32] Wang S, Zeng C, Zhu G, Wang H and Li B 2023 *Phys. Rev. Res.* **5** 043009
[33] Zhan F, Li N, Kohler S and Hänggi P 2009 *Phys. Rev. E* **80** 061115
[34] Li N, Zhan F, Hänggi P and Li B 2009 *Phys. Rev. E* **80** 011125
[35] Ren J and Li B 2010 *Phys. Rev. E* **81** 021111
[36] Wang L and Wu J 2014 *Phys. Rev. E* **89** 012119
[37] He D, Ai B Q, Chan H K and Hu B 2010 *Phys. Rev. E* **81** 041131
[38] Zhong W R, Zhang M P, Ai B Q and Hu B 2011 *Phys. Rev. E* **84** 031130
[39] Yang Y, Ma D, Zhao Y and Zhang L 2020 *J. Appl. Phys.* **127** 195301
[40] Yang Y, Li X and Zhang L 2021 *Chin. Phys. Lett.* **38** 016601
[41] Braun O M and Kivshar Y S 1998 *Phys. Rep.* **306** 1
[42] Hu B, Li B and Zhao H 1998 *Phys. Rev. E* **57** 2992
[43] Ruan Q and Wang L 2020 *Phys. Rev. Res.* **2** 023087
[44] Lepri S, Livi R and Politi A 2003 *Phys. Rep.* **377** 1
[45] Dhar A 2008 *Adv. Phys.* **57** 457
[46] Dhar A, Kundu A and Kundu A 2019 *Front. Phys.* **7** 159